INORGANIC CHEMISTRY

FRONTIERS

Accepted Manuscript

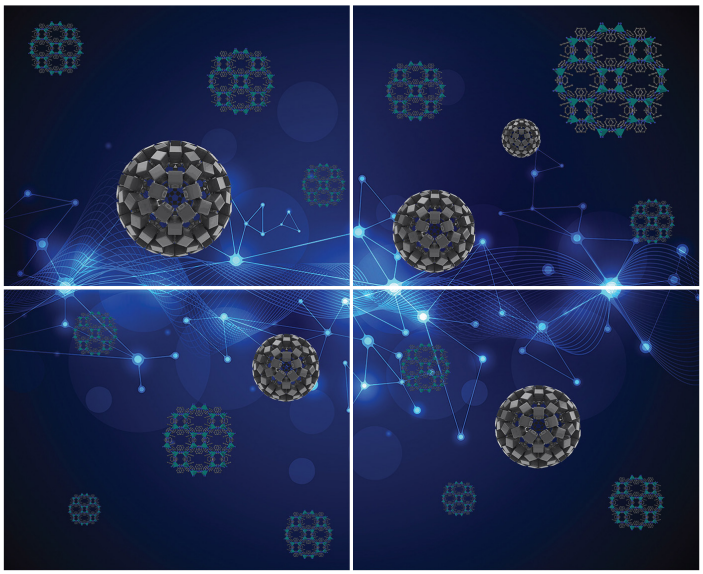

This article can be cited before page numbers have been issued, to do this please use: R. Sánchez-de-Armas and C. J. Calzado, *Inorg. Chem. Front.*, 2022, DOI: 10.1039/D1QI01487K.

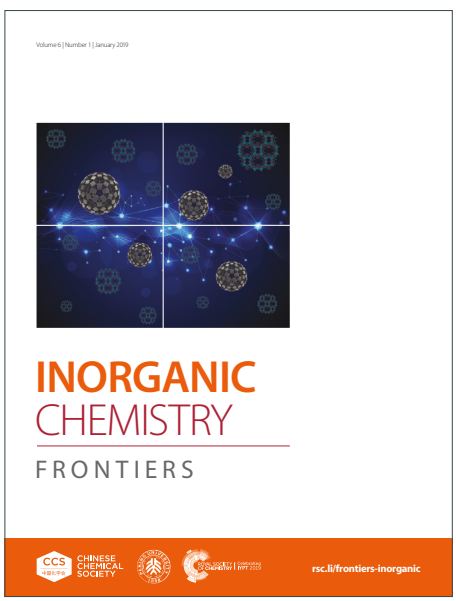

View Article Online
DOI: 10.1039/D1QI01487K

Spin-crossover Fe(II) complexes on surface: the mixture of low-spin and high-spin molecules at low temperature from quantum-chemistry calculations

Rocío Sánchez-de-Armas and Carmen J. Calzado*

Departamento de Química Física. Universidad de Sevilla,
calle Prof. García González, s/n, 41012 Sevilla. Spain.

ABSTRACT

A common feature of spin-crossover molecules deposited on a substrate is the presence of a residual proportion of high-spin (HS) molecules at low temperature, instead of the pure low-spin (LS) phase observed in bulk. In this work, we analyse by means of periodic rPBE calculations, the deposition of a monolayer of the Fe(II) spin-crossover [Fe((3,5-$(CH_3)_2Pz)_3BH)_2$] complex on Au(111) substrate, with different proportion of HS/LS molecules. Our results indicate that there exists both thermodynamic and kinetic factors favoring the presence of the mixed HS/LS state at low temperature. The pure LS phase and a mixed spin state with 1/3 of HS molecules are close in energy, and the transition from this mixed spin state to the pure LS is hindered by the highest activation barrier in the transition from the HS to LS phase. The presence of the surrounding molecules of the 2D superstructure facilitates the transition from the LS to HS state and the interaction between the molecular layer and the surface increases with the proportion of HS molecules, in line with the epitaxial growth of the monolayer and its similarities with the $(01\bar{1})$ plane of the HS bulk molecular crystal. The density of states resulting from the rPBE calculations is used to simulate the STM images. An excellent agreement is found between the simulated STM images for the mixed state with 1/3 of HS molecules and the images acquired at constant height for a submonolayer of this Fe(II) complex on Au(111).

1. INTRODUCTION

Spin-crossover (SCO) compounds have been postulated as potential key components of nanoscale devices due to the possibility of switching between two electronic states under an external perturbation such as light, temperature, electric field, …[1,2,3, 4,5,6, 7] The switch between a low-spin (LS) and a high-spin (HS) state is accompanied with changes in volume, colour, magnetic susceptibility, … properties that can be used to monitor the progress of the transition. Despite their potential, the practical implementation of SCO molecules in nanodevices faces three main challenges: (i) the deposition on the surface of the substrate, without fragmentation and/or decomposition, (ii) the preservation of the spin-crossover properties, and (iii) the enhancement of the intrinsically low conductivity that makes necessary to implement the complex on a conducting matrix.[1-8,9,10] Although different techniques have been employed to deposit the SCO complexes, the sublimation is the most promising one, despite only a small fraction of the large number of synthesized SCO complexes are vacuum-sublimable.[2,6] Moreover, once deposited the molecules can suffer fragmentation, block one of the spin state or present a mixed spin state at low temperature.[5,11] This is the case of the prototypical Fe(II) complex $[Fe((3,5\text{-}(CH_3)_2Pz)_3BH)_2]$, Pz= pyrazolyl, (**Fe-pz**, Figure 1), extensively studied in the recent past.[12,13,14,15,16] In the form of a powder, the molecule presents an asymmetric hysteresis, with transition temperatures of $T_{HS\rightarrow LS}$ =174K and $T_{LS\rightarrow HS}$=199K,[12] 205K.[13,17] When deposited as thick films, monolayer or submonolayer on different substrates (metal surfaces, SiO_2, quartz, ….), it undergoes an incomplete spin transition from the HS state at high-temperature to a mixed-state at low temperature.[13,17,18] In the case of metal surfaces such as Au(111), Cu(111) and Ag(111) the Fe-pz molecules form a long-range superstructure of one-molecule width where both LS and HS states are present.[18,15,19,20,21,22] The composition of this 2D superstructure at low temperature has been described on a series of works of the same group using different experimental techniques. The former works mainly based on scanning tunnelling microscopy (STM), scanning tunnelling spectroscopy (STS) and X-ray absorption spectroscopy (XAS) characterized the 2D superstructure on Au(111) as composed by 66% of LS molecules,[18,15,19,20] while more recent experiments based on X-ray absorption spectroscopy (XAS) supported a composition of 66% of HS molecules.[21,22] Recently, a study of the deposition of Fe-pz on Cu(111) by XAS showed that the fraction of HS molecules at low temperature depends on the layer thickness, the thicker is the film, the lower is the HS fraction. In all cases, the pure LS state at 4K has been discarded, at low temperature a mixture of HS and LS phases is observed. This mixed state at low temperature has also been observed for other molecules on metal surfaces.[23,24] In the case of Fe-pz deposited on Au(111), a mechanoelastic model ascribed this mixed state to the epitaxial relationship of the molecular layer with the metal surface.[20] Also recent Arrhenius Monte Carlo simulations of the interaction of Fe-pz with Cu(111) surface,[22] based on a 3D mechanoelastic model, highlights the role of the substrate on the thermal bistability and HS fraction of Fe-pz ultrathin films.

It is the aim of this work to explore in depth, with the help of state-of-the-art quantum chemistry calculations, the relevance of the intermolecular and molecule-substrate interactions on the relative stability of a Fe-pz monolayer deposited on Au(111), with different fractions of HS molecules. We take benefit from a recent study where the deposition of isolated Fe-pz molecules on Au(111) surface has been analysed, using a combined strategy of periodic DFT and wavefunction-based calculations.[25] These calculations showed that the

View Article Online
DOI: 10.1039/D1QI01487K

isolated LS molecule interacts more strongly with the metal surface than the HS one, and thus this interaction stabilizes in advantage the LS→ HS transition energy. In this work, instead, we explore the deposition of a monolayer with the 2D superstructure previously described from X-ray diffraction measurements.[20,18] The aim of this study is to elucidate whether the presence of intermolecular interactions, at the distances and orientations imposed by the epitaxial growing of the molecular layer on the metal surface, can promote the permanence of a fraction of HS state at low temperature, instead of the pure LS phase observed in the crystal bulk. Our results indicate that the LS→ HS transition energy is remarkably reduced when the molecules form the 2D superstructure, the mixed HS/LS state competes with the pure LS state and the transition from this mixed spin state to the pure LS one is hindered by the highest activation barrier on the HS→ LS conversion. The simulated STM images of the monolayer with 33% of HS molecules reproduce correctly those registered at positive and negative bias voltages for a submonolayer of Fe-pz on Au(111).

2. COMPUTATIONAL DETAILS

We have studied the deposition of a monolayer of the Fe-pz molecule on Au(111) by means of periodic density functional theory (DFT) based calculations, in the frame of the projector-augmented wave (PAW) method.[31,32] In all the calculations, the revised Perdew-Burke-Ernzerhof functional (rPBE)[30] is employed. The choice of the exchange-correlation functional is based on our previous study of the Fe-pz molecule, where we demonstrated that rPBE functional provides estimates of the HS-LS transition energy in excellent agreement with those obtained with wavefunction based calculations such as CASSCF/CASPT2 and NEVPT2.[25] Additionally, benchmark calculations on Fe(II) and Fe(III) SCO complexes have concluded that this functional correctly reproduces the LS-HS transition energy, with better agreement with the experimental estimates than other generalized gradient approximation (GGA) functionals.

A cutoff of 500 eV has been established for the plane-wave basis sets representing the valence electrons, and all the calculations refer to the Γ-point of the Brillouin zone.[34] The lattice parameters of the Au bulk were optimized, the resulting parameters a=b=c=2.97 Å has been used to model the (111) surface. During the optimization of the surface, only the atomic positions of the upper layer were relaxed, while the lattice parameters were restrained to those optimized for the bulk.

The 2D molecular superstructure deposited on gold is modelled with unit cells containing three Fe-pz molecules (Figure 1), where a slab with 144 atoms distributed in 4 layers (19.47 x 15.43 Å) represents the Au(111) surface. In the z direction, the slabs are separated by 30 Å of vacuum that prevent interactions in this direction. The optimized geometry for the different spin states, obtained by Fourmental *et al.*[20] with DFT+U method have been used as starting point in our optimizations. The convergence requirements for the electronic and ionic relaxations are fixed to 10^{-6} eV and 0.025 eV/Å, respectively. That is, the relaxation of the electronic degrees of freedom is stopped when the energy change between two steps is smaller than 10^{-6} eV, while the optimization reaches convergence when all the Hellmann-Feynman forces are lower than 0.025 eV/Å. The NUPDOWN option is used to set the difference between the number of electrons in the up and down spin components, N_α-N_β, and obtain

solutions that represent different fraction of HS molecules on the monolayer. Hence, NUPDOWN is forced to be 0 for the pure LS phase, 4 for the monolayer with 1/3 of HS molecules, 8 for a monolayer with 2/3 of HS molecules and 12 for the pure HS phase. Once optimized, the NUPDOWN restriction is removed, and the total energy of each solution is recalculated. A residual magnetic moment is found on the Fe LS centers ($|m_{Fe}|$~$0.3\mu_\beta$) once the NUPDOWN restriction is removed.

To evaluate the zero-point energy (ZPE) of the HS and LS molecules deposited on Au(111), reduced hessian matrices[35] (i.e., considering only the displacements of the atoms of the Fe-pz molecule and the first layer of gold surface) were calculated at the Γ point for a single Fe-pz molecule deposited on Au(111). Details of the cell employed in these calculations can be found in Ref. [25]. The frequencies of the molecular modes, ν_i, are approximated to the 3N-6 highest ones, and the zero-point energy of each spin state is obtained as: $ZPE_{HS/LS} = \sum_{i=1}^{Nvib} \frac{1}{2} h\nu$

The difference between the ZPE of HS and LS state at this level of calculation is $\Delta ZPE = ZPE_{HS} - ZPE_{LS} = -9.85$ kJ/mol, i.e., zero-point energies favour the HS state. This result is in excellent agreement with benchmark calculations on molecular Fe SCO complexes,[36] showing that the zero-point energies favoured high spin states by -9 kJ/mol on average.

Finally, we have simulated the STM images of the deposited monolayer with two different bias voltage (-1 and 1 V) in the frame of the Tersoff-Hamann approximation.[37] The *p4vasp* program was employed to visualize the STM images in a constant-height mode, using density values of 0.00 and 0.012 e/Å^3 as low and high boundaries, respectively.

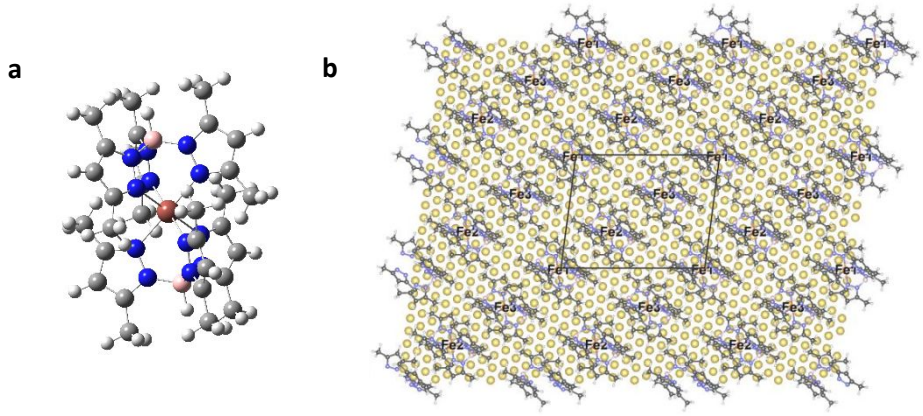

Figure 1. a) [Fe((3,5-$(CH_3)_2$Pz)$_3$BH)$_2$] complex (Fe-pz). b) Top view of the two-dimensional Fe-pz molecular layer deposited on Au(111). The box corresponds to the three-molecule unit cell employed on the calculations. Yellow, brown, pink, blue, gray and white represent, respectively, Au, Fe, B, N, C and H atoms.

3. RESULTS

We have optimized the three-molecule cell deposited on Au(111) surface on different spin states by means of periodic rPBE calculations, where both the Fe-pz molecules and the upper layer of the gold slab are completely relaxed. We used as starting point the optimized geometry for the different spin states, obtained by Fourmental *et al.*[20] with DFT+U method.

View Article Online
DOI: 10.1039/D1QI01487K

During the optimization, the molecules are free to move in the three directions, any constrain has been imposed. Once optimized, no significant displacements on z direction are observed and the 2D molecular layer maintains the epitaxial relationship with the surface, non-significant deviations are found with respect to the x-ray diffraction pattern,[20] corresponding to a monoclinic two-dimensional lattice with parameters $\|\vec{A}\| =$ 9.01±0.04 Å, $\|\vec{B}\| =$ 11.02±0.02 Å, and $\|(\vec{A},\vec{B})\| =$ 81.0±0.2°. It is important to mention that the structure of the molecular layer is close to that of the $(01\bar{1})$ plane of the HS bulk molecular structure.[20] In all cases, the molecule is tilted to the surface, the B-Fe-B axis forming an angle of ~ 20°, in good agreement with the measurements.[20]

Table 1 shows the relative energy of the explored spin solutions once the geometries are optimized. In this table, LSHSHS, for instance, refers to the solution where Fe1, Fe2 and Fe3 centers of the unit cell occupy the LS, HS and HS state, respectively. The most stable solution corresponds to the pure LS state, the energy of the different solutions increases with the fraction of HS molecule. Slightly different energies are found for solutions with 1/3 of HS molecules (LSLSHS and LSHSLS), the same occurs for solutions LSHSHS and HSHSLS, the difference between them give us an estimate of the precision of our calculations.

The pure LS state is separated by only 10.9 kJ/mol to the mixed solution where 1/3 of the molecules are on the HS state (LSLSHS solution). The energy value of 10.9 kJ/mol corresponds to the energy required to switch the spin of 1/3 of the Fe centers from the LS to the HS state and accommodate the coordination sphere of these Fe centers due to the spin change. This transition energy is almost 2.5 times smaller than the energy required for switching the spin of an isolated molecule deposited on gold (25.1 kJ/mol).[25] Then, the presence of the surrounding molecules of the 2D superstructure facilitates the transition from LS to HS state.

A second LS→ HS switch inside this three-molecule cell, that is, going from LSLSHS to LSHSHS is energetically more demanding, about 23 kJ/mol in average. Finally, the energy required for the third LS→ HS switch, i.e. the separation between the solution with 2/3 of molecules on the HS state (LSHSHS) and the pure HS state (HSHSHS) is of 26 kJ/mol. The LS→ HS transition energy evaluated for the bulk molecular crystal at the same level of calculation is of 29.5 kJ/mol. [25] Interestingly, when the HS fraction on the 2D layer increases, the transition energy approaches the bulk value, in line with the similarities found between the structures of the molecular layer and the $(01\bar{1})$ plane of the HS bulk molecular crytal.[20] Then the LS molecules are unfavoured in the monolayer supported on gold, subject to the constrains imposed by the structure of the high-temperature phase. Thus, the LS-HS transition is modulated both by the presence of the surface and by the interaction with surrounding molecules.

Including the zero-point correction energy considerably reduces the separation between the successive transitions (Table 1, ZPE entry). Hence, the pure LS phase and the solution with 1/3 of HS molecules are almost degenerate, in line with the presence of the mixed state at low temperature. The energy difference between the monolayer with 1/3 of HS and 2/3 of HS molecules is now of 14 kJ/mol, and 16 kJ/mol for the separation between 2/3 of HS molecules and only HS molecules on the monolayer.

The role of the interaction with the surface can be evidenced from the comparison with the relative energies of the optimised 2D molecular superstructure *without* including the gold slab. In absence of the surface, the relative energy of the LSLSHS solution with respect to the pure

LS phase is of 19.1 kJ/mol. Hence, the presence of the surface represents a stabilizing factor of about 8 kJ/mol (comparison between 10.9 kJ/mol including gold surface versus 19.1 kJ/mol without surface). For increasing fraction of HS molecules, the interaction with the surface is more important, representing a stabilizing contribution of 11.5 and 13.2 kJ/mol for the HSHSLS and HSHSHS solutions, respectively. Then the higher the fraction of HS molecules on the cell, the stronger the interaction with the surface. This result contrasts with that obtained for isolated molecules on Au(111) surface, where we found a stronger interaction with the surface for LS than HS molecules.[25] Hence, the deposition on a well-ordered monolayer determines the interaction with the surface. Again, this trend can be related to the epitaxial growing of the molecular layer on the metal surface, and the similarities with the $(01\bar{1})$ plane of the HS phase.[20]

Our results indicate that both the presence of the surface and the formation of the molecular superstructure, subject to the epitaxial strain, favour the HS state and it is in line with the existence of a mixed spin state at low temperature. Moreover, the reduction of the transition energy for the deposited molecules on the 2D superstructure is in agreement with the behaviour found for thick Fe-pz films deposited on Si(100)/SiO_2 and quartz, where the transition temperatures shifted towards lower values when the film thickness decreased.[12] The same trends have been observed for Fe-pz on Cu(111).[22]

Table 1. Relative energy (in kJ/mol) for the different spin state distributions for three molecules per unit cell forming the 2D superstructure on Au(111) surface. ZPE entries refer to the relative energy including the zero-point energy correction. The relative energy of the single molecule deposited on surface in the LS and HS states is also included for comparison, as well as the relative energy of the molecular crystal resulting from rPBE calculations.[25]

Coverage	Pure LS	33% HS		66% HS		Pure HS
	LSLSLS	LSLSHS	LSHSLS	LSHSHS	HSHSLS	HSHSHS
3 molecules/cell on Au(111)	0.0	10.9	11.6	35.2	33.1	60.2
+ZPE	0.0	1.0	1.7	15.5	13.4	30.5
3molecules/cell without substrate	0.0	19.1	19.1	---	44.6	73.4
1 molecule/cell	0.0					25.1
+ZPE	0.0					15.2
molecular crystal[25]	0.0					29.5

Additional insight can be obtained from the evaluation of the energy barriers for the spin transition inside the 2D molecular layer. A set of intermediate structures were generated by interpolation from the optimized LSLSLS, LSLSHS, LSHSHS and HSHSHS solutions of the 2D layer on gold, the same procedure we have employed to study the LIESST phenomena on Fe-pz molecule.[25] Each intermediate structure represents the geometrical midpoint between two optimized solutions. The relative energy of these intermediates is represented in Figure 2. Since our calculations do not take into account spin-orbit effects, the blue line in this figure is just a guide to the eye. Interestingly, the transition from the pure HS phase to a mixed state

View Article Online
DOI: 10.1039/D1QI01487K

with 2/3 of HS molecules (LSHSHS) proceeds without activation barrier. In the next step, from a state with 2/3 of HS (LSHSHS) to a 1/3 of HS (LSLSHS), the barrier is about 6 kJ/mol, while the barrier doubles in the last step, from LSLSHS to the pure LS phase. Then by cooling, the barrier increases and the thermal energy decreases, the spin transition becomes more and more kinetically hindered. In summary, our calculations demonstrate that there exist thermodynamic and kinetic factors favouring the presence of a mixed-spin state at low temperature. Thus, the pure LS phase and the mixed phase (with 66% of LS molecules) are close in energy and the transition from this mixed phase to the pure LS one presents the highest activation barrier.

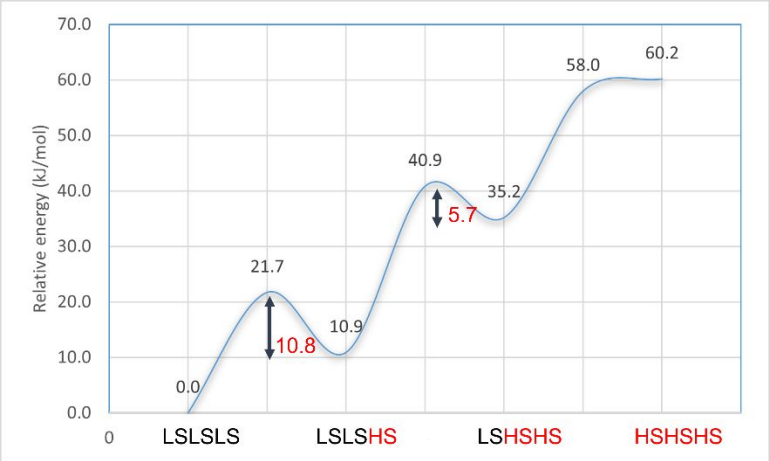

Figure 2. Relative energy (in kJ/mol) for the different spin solutions of the 2D molecular layer deposited on Au(111). The zero-point energies are not included. The activation barriers for the successive spin transitions on cooling are indicated in red.

Finally, we can use the density of states (DOS) resulting from our rPBE calculations to interpret the STM images acquired for a submonolayer coverage of Fe-pz molecules on Au(111) substrate, at positive (0.3V) and negative (-0.7 V) bias voltage (Figure 4). For positive bias, V, the electrons flow from the STM tip to the empty orbitals of the sample, placed between the Fermi level E_F and E_F+V. Since the tip is placed on the top of the molecule, the local states accessible for the tip electrons are those centered on the molecule. For negative bias, the electrons flow from the occupied orbitals of the sample to the tip, and the STM images provided then information about the local states of the molecule placed between E_F and E_F-V.
The projected DOS on Fe centers shows that the 3d Fe orbitals are close to the Fermi level in all the explored situations (Figure 3). The unoccupied Fe d orbitals are higher in energy for LS than HS state, placed about 2 eV above the Fermi level in the case of LS state, and 0.5 eV in HS molecules. Similar results are obtained with DFT+U approach.[18,20] This agrees with the strength of the ligand field on Fe site, stronger for LS than HS state. Hence, the energy splitting of the t_{2g} and e_g-like orbitals is then larger for LS than HS molecules. In the case of Fe-pz molecule, the separation between the barycentres of the t_{2g} and e_g-like orbitals, evaluated by mean of ab initio ligand field theory approach, is of 16189 cm^{-1} for the LS molecule and 9523 cm^{-1} for the HS state.[25] Additionally, the energy distribution of these Fe 3d unoccupied orbitals is coherent

View Article Online
DOI: 10.1039/D1QI01487K

with the spin-dependent Fe L_3 edge of the X-ray absorption spectra, which requires photons of higher energy for LS (708.0 eV) than for HS state (double peak at 706.7 and 707.9 eV). The L_3 edge corresponds to $2p^{3/2} \rightarrow$ d transitions, and since the core levels are independent of the spin state, these transitions reflect the energy distribution of the unoccupied d orbitals.[11]

Additionally, the projected DOS on Fe and ligands for the pure phases show a larger hybridization with the ligands for the LS phase than for the HS one, in line with the strength of the Fe ligand field. In fact, for the low temperature phase, where the LS state is favored, the Fe-N distances are shorter and the mixing between the Fe 3d and the ligand-center orbitals is stronger than in the case of the high temperature phase. The mixed phases with 1/3 and 2/3 of HS molecules show features of both limit situations. They present similar shape, only differ by the density of states at each energy. The projected DOS on Fe centers allow to distinguish the minority spin on each case (green dashed area in Figure 3), and to identify the electronic state of the Fe centers probed by the STM tip.

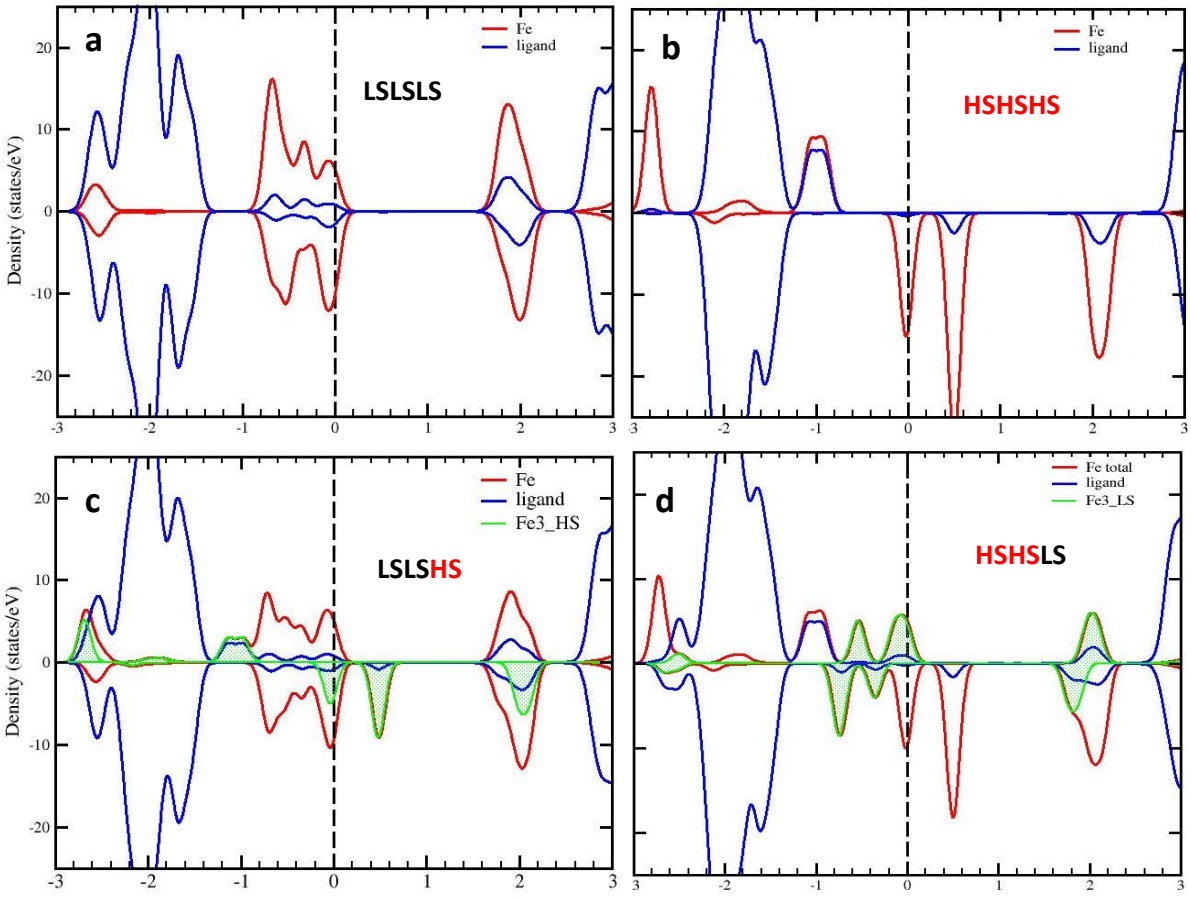

Figure 3. Density of states projected on Fe sites (red) and ligands (blue) for the different solutions, the pure phases (a) LSLSLS and (b) HSHSHS, and mixed phases (c) LSLSHS, (d) HSHSLS. In mixed phases, the green line and dashed area corresponds to the DOS projected on the Fe site with minority spin state.

View Article Online
DOI: 10.1039/D1QI01487K

Experimentally, STM images were acquired at 0.3V and -0.7V in constant heigh mode for a submonolayer of Fe-pz on Au(111)[18] (Figures 4a and 4b). The red box represents a three-molecule unit cell, with the $S_{1/3}$ superstructure described in Ref. 18. With a negative bias voltage of -0.7 V, only two of the three molecules of the unit cell appear as bright spots, with more negative bias (V= -1.5 V in Figure 1 of Ref 18) the third molecule is also visible, although less bright than the other two. At a positive bias of 0.3 V, only one molecule over three appears bright. We have simulated the STM images using the density of states provided by the calculations at bias of +1V and -1V. In positive bias, only the HS molecules can be imaged by STM, since the low-lying unoccupied states of the LS molecules appear at about 2 eV (Figure 3). However, in negative bias, both molecules can be probed by STM, since the Fe-pz molecules present occupied states close to the Fermi level independently of the spin state. At positive bias (Figures 4c and 4e) only the HS molecules appears as bright spots, while for negative bias, the spots are brighter for the LS molecules than for the HS ones (Figures 4d and 4f), in line with the higher density of states of LS molecules. The comparison with the experimental images indicates a nice agreement with the simulated STM images of the monolayer containing 1/3 of HS molecules.

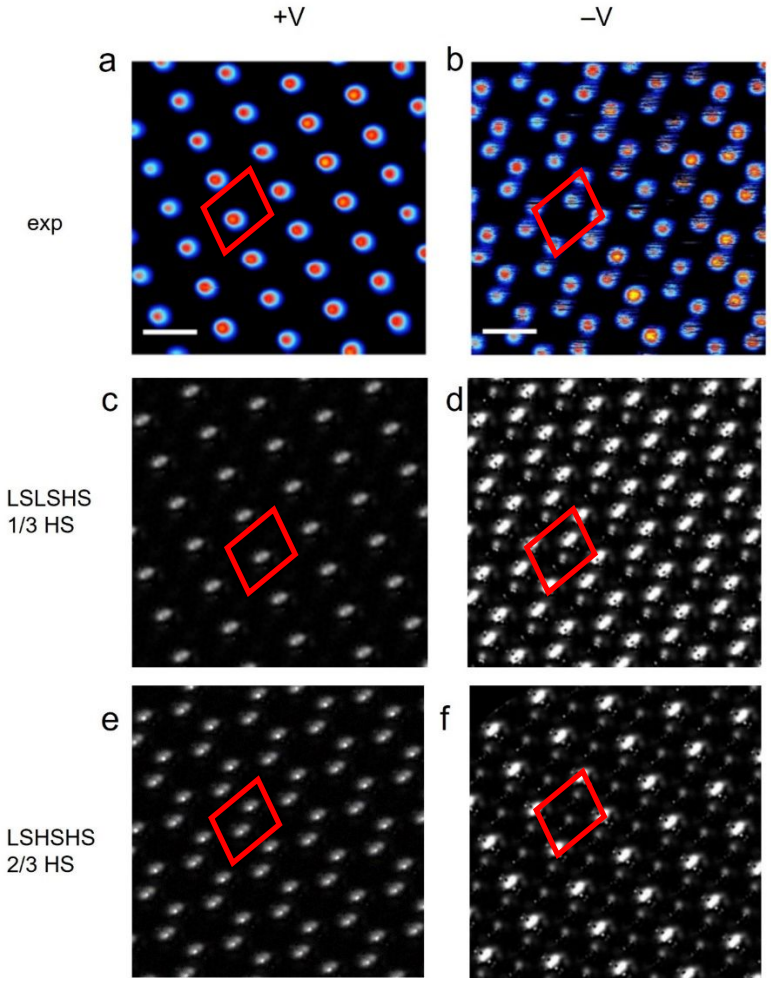

Figure 4. Constant height STM images recorded at +0.3V (a) and -0.7V (b) for the same area of a submonolayer of Fe-pz molecules on Au(111) surface (⟨ I ⟩ =50pA). The scale bars correspond to 2nm in both images. From Ref. [18] , supplementary Figure 3. Simulated constant height STM images at +1V (c) and -1V (d) for LSLSHS solution, and +1V (e) and -1V (f) for LSHSHS phase. The red box represents the three-molecule unit cell employed in the calculations. For ease of comparison, the box is also included in the experimental STM images (a,b).

4. CONCLUSIONS

The presence of a residual HS fraction at low temperature on thin films and monolayers of SCO complexes seems to be a common feature accompanying the deposition of SCO complexes on substrates of different nature.[38,39,40,24,41] The origin of this behaviour has been ascribed to epitaxial strain and a related loss of cooperativity.[42,21,20,41] Previous studies based on mechanoelastic models confirmed the role played by the substrate on the spin-crossover transition. [20,22] This work goes one step further analysing the deposition by means of periodic DFT calculations, that explicitly take into account the structural and electronic effects involved in the molecule-molecule interactions inside the monolayer and governing the interaction with the surface. We have determined by means of periodic DFT calculations the relative stability of a structured monolayer of the Fe-pz complex on Au(111) with different proportion of HS molecules. Our calculations indicate that the mixed state with a 33% of HS molecules and the pure LS phase are almost degenerate and the monolayer-surface interaction increases with the HS proportion on the monolayer, in line with the fact that the monolayer presents a structure close to the $(01\bar{1})$ plane of the HS bulk molecular crystal. Indeed, the transition from this mixed phase to the pure LS one shows the highest activation barrier on cooling from HS to LS phase. All these factors favour the presence of a non-negligible fraction of HS molecules on the molecular layer at low temperature, as observed experimentally. Although this study is devoted to the deposition of the Fe-pz complex on Au(111) surface, these results could be also useful to other SCO complexes in direct contact with the substrate and a residual fraction of HS molecules at low temperature.

As an additional proof of the reliability of our calculations, we have simulated the STM images using the density of states provided by the rPBE calculations. We find that the simulated images of the monolayer with 33% of HS molecules reproduce correctly the STM images recorded on islands of one-molecule height deposited on Au(111).

CONFLICTS OF INTEREST

There are no conflicts of interest to declare.

ACKNOWLEDGMENTS

The authors acknowledge the financial support through grant PGC2018-101689-B-I00 funded by MCIN/AEI/ 10.13039/501100011033 and by “ERDF A way of making Europe”. The authors thank Dr. C. Barreteau for providing us with the optimized geometries at LDA+U level of the deposited molecules on Au(111) surface, reported in Ref. 20, here used as starting point

View Article Online
DOI: 10.1039/D1QI01487K

in the rPBE optimizations. The technical support of the Supercomputing Team of the Centro Informático Científico de Andalucía (CICA) and the access to the computational facilities of the "Centro de Servicios de Informática y Redes de Comunicaciones" (CSIRC, Universidad de Granada, Spain) are also acknowledged.

REFERENCES

1. Gütlich, P.; Hauser, A.; Spiering, H., Thermal and Optical Switching of Iron(II) Complexes. *Angew. Chem. Int. Ed.* **1994,** *33*, 2024-2054.
2. Kumar, K. S.; Ruben, M., Sublimable Spin-Crossover Complexes: From Spin-State Switching to Molecular Devices. *Angew. Chem. Int. Ed.* **2021,** *60*, 7502-7521.
3. Kumar, K. S.; Ruben, M., Emerging trends in spin crossover (SCO) based functional materials and devices. *Coord. Chem. Rev.***2017,** *346*, 176-205.
4. Bousseksou, A.; Molnar, G.; Salmon, L.; Nicolazzi, W., Molecular spin crossover phenomenon: recent achievements and prospects. *Chem. Soc. Rev.***2011,** *40*, 3313-3335.
5. Molnar, G.; Rat, S.; Salmon, L.; Nicolazzi, W.; Bousseksou, A., Spin Crossover Nanomaterials: From Fundamental Concepts to Devices. *Adv. Mater.* **2018,** *30*, 17003862.
6. Kipgen, L.; Bernien, M.; Tuczek, F.; Kuch, W., Spin-Crossover Molecules on Surfaces: From Isolated Molecules to Ultrathin Films. *Adv. Mater.* **2021,** *33*, 2008141.
7. Cannizzo, A.; Milne, C.; Consani, C.; Gawelda, W.; Bressler, C.; van Mourik, F.; Chergui, M., Light-induced spin crossover in Fe(II)-based complexes: The full photocycle unraveled by ultrafast optical and X-ray spectroscopies. *Coord. Chem. Rev.***2010,** *254*, 2677-2686.
8. Kumar, K.; Salitros, I; Boubegtiten-Fezoua, Z.; Modovan, S.; Hellwig, P.; Ruben, M. A spin crossover(SCO) active graphene-iron(II) complex hybrid material. *Dalton Trans*. **2018**, *47*, 35-40.
9. Koo, Y.; Galan-Mascaros, J., Spin Crossover Probes Confer Multistability to Organic Conducting Polymers. *Adv. Mater.* **2014,** *26*, 6785-6789.
10. Qiu, D.; Ren, D. H.; Gu, L.; Sun, X. L.; Qu, T. T.; Gu, Z. G.; Li, Z. J., Spin crossover-graphene nanocomposites: facile syntheses, characterization, and magnetic properties. *RSC Advances* **2014,** *4* , 31323-31327.
11. Gruber, M.; Berndt, R., Spin-Crossover Complexes in Direct Contact with Surfaces. *Magnetochemistry* **2020,** *6*, 26.
12. Davesne, V.; Gruber, M.; Studniarek, M.; Doh, W. H.; Zafeiratos, S.; Joly, L.; Sirotti, F.; Silly, M. G.; Gaspar, A. B.; Real, J. A.; Schmerber, G.; Bowen, M.; Weber, W.; Boukari, S.; Costa, V. D.; Arabski, J.; Wulfhekel, W.; Beaurepaire, E., Hysteresis and change of transition temperature in thin films of Fe{[Me2Pyrz]3BH}2, a new sublimable spin-crossover molecule. *J. Chem. Phys.* **2015,** *142*, 194702.
13. Iasco, O.; Boillot, M. L.; Bellec, A.; Guillot, R.; Rivière, E.; Mazerat, S.; Nowak, S.; Morineau, D.; Brosseau, A.; Miserque, F.; Repain, V.; Mallah, T., The disentangling of hysteretic spin transition, polymorphism and metastability in bistable thin films formed by sublimation of bis(scorpionate) Fe(ii) molecules. *J. Mater. Chem. C* **2017,** *5*, 11067-11075.
14. Kelai, M.; Cahier, B.; Atanasov, M.; Neese, F.; Tong, Y.; Zhang, L.; Bellec, A.; Iasco, O.; Riviere, E.; Guillot, R.; Chacon, C.; Girard, Y.; Lagoute, J.; Rousset, S.; Repain, V.; Otero, E.; Arrio, M.; Sainctavit, P.; Barra, A.; Boillot, M.; Mallah, T., Robust magnetic anisotropy of a monolayer of hexacoordinate Fe(ii) complexes assembled on Cu(111). *Inorg Chem. Front.* **2021,** *8*, 2395-2404.

15. Bairagi, K.; Bellec, A.; Fourmental, C.; Iasco, O.; Lagoute, J.; Chacon, C.; Girard, Y.; Rousset, S.; Choueikani, F.; Otero, E.; Ohresser, P.; Sainctavit, P.; Boillot, M.; Mallah, T.; Repain, V., Temperature-, Light-, and Soft X-ray-Induced Spin Crossover in a Single Layer of Fe-II-Pyrazolylborate Molecules in Direct Contact with Gold. *J. Phys. Chem. C* **2018,** *122*, 727-731.

16. Konstantinov, N.; Tauzin, A.; Noumbe, U.; Dragoe, D.; Kundys, B.; Majjad, H.; Brosseau, A.; Lenertz, M.; Singh, A.; Berciaud, S.; Boillot, M.; Doudin, B.; Mallah, T.; Dayen, J., Electrical read-out of light-induced spin transition in thin film spin crossover/graphene heterostructures. *J. Mater. Chem. C* **2021,** *9,*2712-2720.

17. Bairagi, K.; Bellec, A.; Fourmental, C.; Iasco, O.; Lagoute, J.; Chacon, C.; Girard, Y.; Rousset, S.; Choueikani, F.; Otero, E.; Ohresser, P.; Sainctavit, P.; Boillot, M.-L.; Mallah, T.; Repain, V., Temperature-, Light-, and Soft X-ray-Induced Spin Crossover in a Single Layer of FeII-Pyrazolylborate Molecules in Direct Contact with Gold. *J. Phys. Chem. C* **2018,** *122*, 727-731.

18. Bairagi, K.; Iasco, O.; Bellec, A.; Kartsev, A.; Li, D.; Lagoute, J.; Chacon, C.; Girard, Y.; Rousset, S.; Miserque, F.; Dappe, Y.; Smogunov, A.; Barreteau, C.; Boillot, M.; Mallah, T.; Repain, V., Molecular-scale dynamics of light-induced spin cross-over in a two-dimensional layer. *Nat. Comm.* **2016,** *7*, 12212.

19. Bairagi, K.; Bellec, A.; Fourmental, C.; Tong, Y.; Iasco, O.; Lagoute, J.; Chacon, C.; Girard, Y.; Rousset, S.; Choueikani, F.; Otero, E.; Ohresser, P.; Sainctavit, P.; Boillot, M.; Mallah, T.; Repain, V., Temperature-, Light-, and Soft X-ray-Induced Spin Crossover in a Single Layer of Fe-II-Pyrazolylborate Molecules in Direct Contact with Gold (vol 122, pg 727, 2018). *J. Phys. Chem. C* **2018,** *122* 29080-29080.

20. Fourmental, C.; Mondal, S.; Banerjee, R.; Bellec, A.; Garreau, Y.; Coati, A.; Chacon, C.; Girard, Y.; Lagoute, J.; Rousset, S.; Boillot, M. L.; Mallah, T.; Enachescu, C.; Barreteau, C.; Dappe, Y. J.; Smogunov, A.; Narasimhan, S.; Repain, V., Importance of Epitaxial Strain at a Spin-Crossover Molecule-Metal Interface. *J. Phys Chem. Lett.* **2019,** *10*, 4103-4109.

21. Zhang, L.; Tong, Y.; Kelai, M.; Bellec, A.; Lagoute, J.; Chacon, C.; Girard, Y.; Rousset, S.; Boillot, M.; Riviere, E.; Mallah, T.; Otero, E.; Arrio, M.; Sainctavit, P.; Repain, V., Anomalous Light-Induced Spin-State Switching for Iron(II) Spin-Crossover Molecules in Direct Contact with Metal Surfaces. *Angew Chem. Int. Ed.* **2020,** *59*, 13341-13346.

22. Kelai, M.; Repain, V.; Tauzin, A.; Li, W.; Girard, Y.; Lagoute, J.; Rousset, S.; Otero, E.; Sainctavit, P.; Arrio, M.; Boillot, M.; Mallah, T.; Enachescu, C.; Bellec, A., Thermal Bistability of an Ultrathin Film of Iron(II) Spin-Crossover Molecules Directly Adsorbed on a Metal Surface. *J. Phys. Chem. Lett.* **2021,** *12*, 6152-6158.

23. Beniwal, S.; Zhang, X.; Mu, S.; Naim, A.; Rosa, P.; Chastanet, G.; Letard, J.; Liu, J.; Sterbinsky, G.; Arena, D.; Dowben, P.; Enders, A., Surface-induced spin state locking of the [Fe(H2B(pz)(2))(2)(bipy)] spin crossover complex. *J. Phys. Condens. Matter.* **2016,** *28*, 206002.

24. Warner, B.; Oberg, J.; Gill, T.; El Hallak, F.; Hirjibehedin, C.; Serri, M.; Heutz, S.; Arrio, M.; Sainctavit, P.; Mannini, M.; Poneti, G.; Sessoli, R.; Rosa, P., Temperature- and Light-Induced Spin Crossover Observed by X-ray Spectroscopy on Isolated Fe(II) Complexes on Gold J. Phys. Chem. Lett. **2013,** *4*, 1546-1552.

25. Montenegro-Pohlhammer, N.; Sanchez-de-Armas, R.; Calzado, C., Deposition of the Spin Crossover Fe-II-Pyrazolylborate Complex on Au(111) Surface at the Molecular Level. *Chem. Eur. J.* **2021,** *27*, 712-723.

26. Kresse, G. H., J., Ab initio molecular dynamics for liquid metals. *Phys. Rev. B* **1993,** *47*, 4.

27. Kresse, G.; Hafner, J., Ab Initio Molecular-Dynamics Simulation of the Liquid-Metal-Amorphous Semiconductor Transition in Germanium. *Phys. Rev. B* **1994,** *49* (20), 14251-14269.

28. Kresse, G.; Furthmuller, J., Efficiency of ab-initio total energy calculations for metals and semiconductors using a plane-wave basis set. *Computational Materials Science* **1996,** *6* (1), 15-50.

View Article Online
DOI: 10.1039/D1QI01487K

29. Kresse, G.; Furthmuller, J., Efficient iterative schemes for ab initio total-energy calculations using a plane-wave basis set. *Phys. Rev. B* **1996,** *54*, 11169-11186.
30. Hammer, B.; Hansen, L. B.; Norskov, J. K., Improved adsorption energetics within density-functional theory using revised Perdew-Burke-Ernzerhof functionals. *Phys. Rev. B* **1999,** *59*, 7413-7421.
31. Blochl, P. E., Projector augmented-wave method. *Phys. Rev. B* **1994,** *50*, 17953-17979.
32. Kresse, G.; Joubert, D., From ultrasoft pseudopotentials to the projector augmented-wave method. *Phys. Rev. B* **1999,** *59*, 1758-1775.
33. Siig, O. S.; Kepp, K. P., Iron(II) and Iron(III) Spin Crossover: Toward an Optimal Density Functional. *J. Phys. Chem. A* **2018,** *122*, 4208-4217.
34. Monkhorst, H. J.; Pack, J. D., Special Points for Brillouin-zone Integrations. *Phys. Rev. B* **1976,** *13* (12), 5188-5192.
35. Bondì, L.; Brooker, S.; Totti, F., Accurate prediction of pressure and temperature T1/2 variation in solid state spin crossover by ab initio methods: the [CoII(dpzca)2] case *J. Matter. Chem. C* **2021,** *9*, 14256-14268.
36. Kepp, K., Theoretical Study of Spin Crossover in 30 Iron Complexes. *Inorg. Chem.* **2016,** *55*, 2717-2727.
37. Tersoff, J.; Hamann, D. R., Theory of the scanning tunneling microscope. *Phys. Rev. B* **1985,** *31*, 805-813.
38. Miyamachi, T.; Gruber, M.; Davesne, V.; Bowen, M.; Boukari, S.; Joly, L.; Scheurer, F.; Rogez, G.; Yamada, T. K.; Ohresser, P.; Beaurepaire, E.; Wulfhekel, W., Robust spin crossover and memristance across a single molecule. *Nat. Commun.* **2012,** *3*, 938.
39. Gruber, M.; Miyamachi, T.; Davesne, V.; Bowen, M.; Boukari, S.; Wulfhekel, W.; Alouani, M.; Beaurepaire, E., Spin crossover in Fe(phen)2(NCS)2 complexes on metallic surfaces. *J. Chem. Phys.* **2017,** *146*, 092312.
40. Pronschinske, A.; Chen, Y.; Lewis, G. F.; Shultz, D. A.; Calzolari, A.; Buongiorno Nardelli, M.; Dougherty, D. B., Modification of Molecular Spin Crossover in Ultrathin Films. *Nano Lett.* **2013,** *13*, 1429-1434.
41. Ossinger, S.; Naggert, H.; Kipgen, L.; Jasper-Toennies, T.; Rai, A.; Rudnik, J.; Nickel, F.; Arruda, L. M.; Bernien, M.; Kuch, W.; Berndt, R.; Tuczek, F., Vacuum-Evaporable Spin-Crossover Complexes in Direct Contact with a Solid Surface: Bismuth versus Gold. *J. Phys. Chem. C* **2017,** *121*, 1210-1219.
42. Rohlf, S.; Grunwald, J.; Jasper-Toennies, T.; Johannsen, S.; Diekmann, F.; Studniarek, M.; Berndt, R.; Tuczek, F.; Rossnagel, K.; Gruber, M., Influence of Substrate Electronic Properties on the Integrity and Functionality of an Adsorbed Fe(II) Spin-Crossover Compound. *J. Phys. Chem. C* **2019,** *123*, 17774-17780.